EFFECTS OF LONG -TERM HIGH TEMPERATURE EXPOSURE ON THE MICROSTRUCTURE OF HAYNES ALLOY 230

J. Veverková[1], A. Strang[1], G.R. Marchant[2] and H.V. Atkinson[1]

1- Department of Engineering, University of Leicester, University Rd., Leicester, LE1 7RH, UK (hva2@le.ac.uk)

2- Siemens Industrial Turbomachinery Ltd, Lincoln, UK (geoff.marchant@siemens.com)

Abstract

Haynes Alloy 230 was specifically designed to have excellent long-term thermal stability and resistance to the precipitation of damaging phases.

This paper describes in detail studies on the effects of long-term high temperature exposure on the hardness, microstructural changes and tensile properties of thermally exposed samples of Haynes Alloy 230. The samples from the 2mm thick sheet material have been investigated using X-Ray diffraction and advanced electron microscopy techniques (FEGSEM, TEM etc.). The evolution of the precipitating phases was monitored across a wide range of temperatures (from 500°C to 1170°C) and durations (from 24 hours up to 30000 hours) and several key phases have been identified. In addition to the primary W-rich carbide and the precipitation of Cr-rich $M_{23}C_6$, a new brittle phase/carbide was observed within the microstructure at the highest exposure temperatures (above 930°C).

The microstructurally based model assists in the assessment of in-service operating temperatures as a means of evaluating the remaining operational life of the components.

Keywords - HA230, microstructural evolution, thermal ageing, hardness, tensile testing

1. Introduction

Haynes Alloy 230™ (HA230) is a solid solution strengthened nickel-based alloy used for combustion components in industrial gas turbines. These components must demonstrate an extended operational life-time at high temperature exposures (with and without mechanical loading) without structural failures. High temperatures together with cyclic mechanical and thermal stresses during long periods of operating service lead to degradation of the microstructure of the alloy and consequently to its mechanical properties. It is important to develop understanding of these processes in order to optimise performance.

Haynes Alloy 230™ has a combination of high temperature strength, long-term thermal stability and outstanding corrosion resistance in oxidising and nitriding environments at service temperatures up to 1150°C. These properties, together with its good formability and weldability characteristics, have made HA230 an ideal material for many aerospace and power industry applications [1].

The alloy was originally developed from the Ni-Cr-Mo-W system with the high nickel content providing a stable austenitic matrix, tungsten effective solid solution strengthening and carbon promoting the formation of chromium rich $M_{23}C_6$ carbide. A range of studies are available in the literature [2-8].

2. Experimental procedure

HA230 for testing was provided by Siemens Industrial Turbomachinery Ltd (SIT) in the form of 2mm thick sheet. All the specimens were taken from this single heat of HA230 (No 8305-5-7170) supplied in the solution treated and quenched condition by Haynes International Ltd to the specification AMS 5838. The chemical composition of the material is shown in *Table 1*.

Table 1 Test certificate: Chemical analysis (wt%) of as-supplied material provided by Haynes Intl..

Heat	Ni	Cr	W	Mo	Fe	Co	Mn	Si	Al	C	La	B
8305-5-7170	Bal	21.75	13.96	1.32	1.40	0.37	0.49	0.36	0.29	0.12	0.013	0.004
AMS 5878	Bal	20.0 to 24.0	13.00 to 15.00	1.00 to 3.00	3.00 max	5.00 max	0.30 to 1.00	0.25 to 0.75	0.20 to 0.50	0.05 to 0.15	0.005 to 0.05	0.015 max

The coupons were thermally exposed in still air at temperatures in the range of 500-1170°C and for duration from 24 hours up to 30000 hours. The microsections were mounted and firstly ground to 600 grit finish for hardness tests and then prepared for metallurgical review by polishing to a 1μm finish and etching in hydrofluoric acid. The microsections were examined using optical microscopy and FEGSEM.

Tensile testing was performed at room temperature on the 3000, 10000, and 20000 hours thermally exposed specimens. The specimens were exposed at six different temperatures (750°C, 810°C, 870°C, 930°C, 990°C, and 1050°C) for all three durations of exposure. The heat treated specimens were cut into the form shown in *Figure 1*, using a milling machine. The summary of all the tests performed is presented in *Figure 2*.

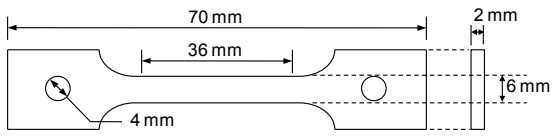

Figure 1 Design of the tensile specimen.

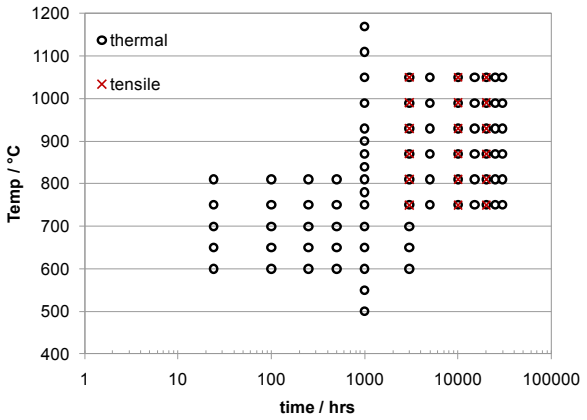

Figure 2 Overview of the tests performed.

3. Result and discussion

3.1. Hardness studies

Vickers hardness tests have been carried out at a load of 20kg along the length of the microsection of unstressed coupons of HA230. The average hardness value of as-received unexposed material was 218 ± 2 Vickers.

The hardness testing provided useful information about the behaviour of the alloy with increasing exposure time and temperature. *Figure 3a* shows hardness variation with time. The specimens exposed at 750°C demonstrate a stable behaviour with only a small fall observed over 30000 hours. For the rest of the exposure temperatures, the primary drop in hardness happens after 1000 hours and then for longer exposures the hardness stays quite stable. The lowest values were obtained for 990°C. In the case of 1050°C the hardness is slowly increasing with exposure time.

One of the aims of this project was to create a Master Curve of Hardness vs. Larson-Miller Parameter (LMP) as a first step in evaluation (i.e. the estimation of the average operating temperature) of ex-service components.

The hardness values are shown in the form of a parametric Larson–Miller plot (see *Figure 3b)*, using a C-value of 20 for the Larson-Miller constant. The results indicate that systematic changes in the hardness of the HA230 occur with increasing temperature and exposure duration.

It is evident from the data curve that the material initially hardens from the original solution annealed value of 218 Vickers to a peak value of the curve of about 246 Vickers and LMP=22. Then re-softening of the alloy occurs reaching its original hardness value at LMP equal to 27.5 approximately. All the curves reach a minimum at a temperature of about 990°C. The minimum value was about 208 Vickers and LMP=30. With additional increase of temperature the material hardens again. The maximum hardness value was obtained for the specimen thermally exposed for 1000 hours at 750°C and the minimum value after exposure of 3000 hours at 990°C.

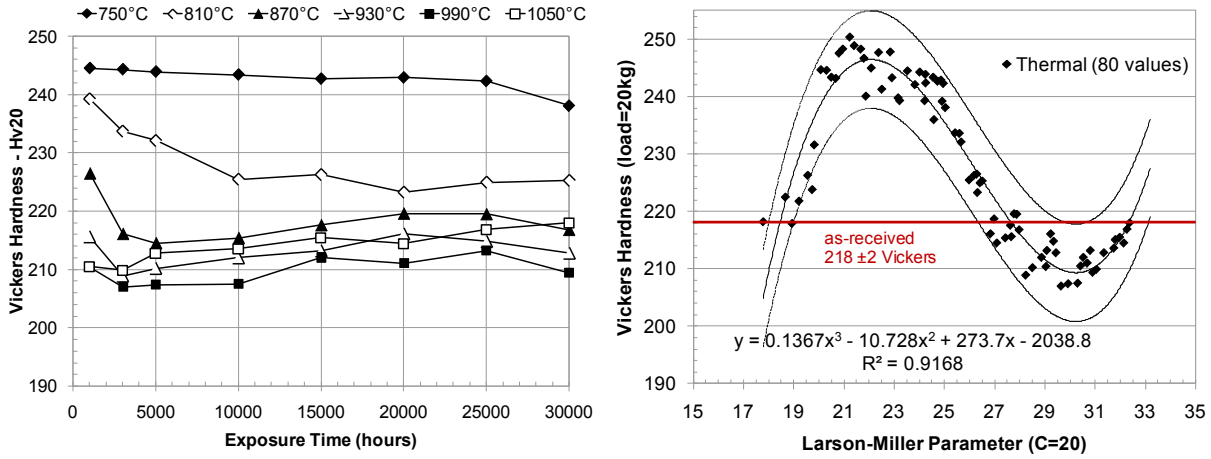

Figure 3 a) Variation of hardness with exposure time for temperatures in the range 750°C -1050°C. b) Hardness data for HA230 thermally exposed coupons plotted versus Larson-Miller parameter. Dotted lines represent the 95% prediction interval.

To analyse the hardness data a least squares regression analysis was used. A good fit for the data set plotted in Figure 3b is obtained using a cubic polynomial of the form $Hv = aP^3 + bP^2 + cP + d$, where a, b, c, and d are constants, Hv is a hardness value and P is the Larson-Miller parameter defined as $P = (273 + T)(20 + \log t)/1000$. The regression constants and R^2 value for hardness data obtained in the project are in *Figure 3b*.

3.1.1. Statistical analysis

The set for the statistical analysis contained 80 hardness values of thermally exposed samples. The sample thermally exposed for 1000 hrs at 1170 (203 Vickers) has been excluded from the calculation. Using 80 observations the 95% confidence interval (CI) and prediction interval (PI) (*Figure 3b*) were calculated. Only two low temperature observations (LMP=19.48 and 21.76) have untypical behaviour. The maximal width of the confidence interval is 3.7 and the maximal width of the prediction interval is equal to 17. The method of maximum likelihood was used for the determination of the optimum value for the LMP constant C. For thermally exposed samples (80 observations) 95% confidence interval for C is 15.1 to 25.5 with the optimum value equal to 19.3. The new optimum value of C (LMP constant) was used to replot the hardness values. The R^2 values change little. Any differences can only be observed in the fourth decimal place. The LMP constant equal to 19.3 made the R^2 value of the 'thermal' set increase from 0.9168 to 0.9169.

3.2. Microstructural studies

Metallographic studies of the microstructure of HA230 are based on an evaluation of images obtained by light optical microscopy and scanning electron microscopy.

3.2.1. As-received HA230

Figure 4 shows the microstructure of the as-received solution treated and quenched HA230 taken from the same batch as for all the coupons for thermal exposure. It contains primary carbides which were identified by X-Ray Diffraction as $M_{12}C$, in the literature usually presented as M_6C type carbides, *e.g.* [2-4, 6-8]. Primary carbides are tungsten rich (see below), equiaxed in shape, sometimes associated with grain boundaries, also dispersed throughout the microstructure in the form of stringers. Any other precipitation has not been identified at this stage. Grains can be identified as equiaxed in the range of ASTM 4-6.

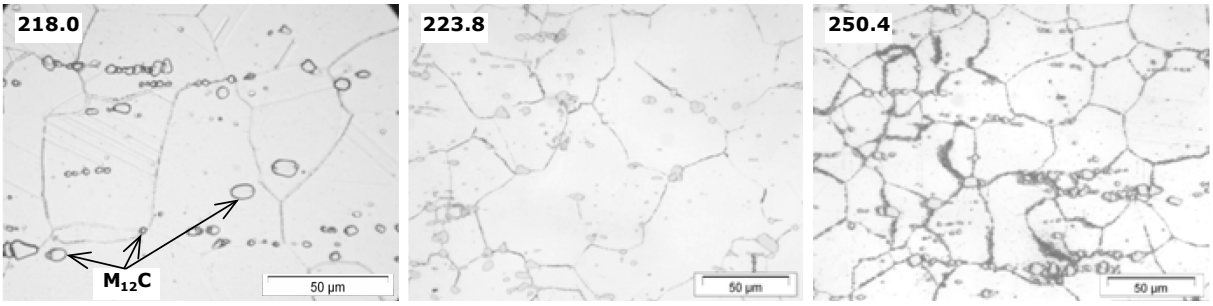

Figure 4 Microstructure of (left to right) annealed and quenched HA230 showing primary carbides; specimen thermally exposed for 24 hours at 650°C; and specimen thermally exposed for 1000 hours at 650°C. The hardness value is given in the top left hand corner.

3.2.2. Thermally Exposed HA230

The microstructural examination was conducted on the thermally exposed HA230 coupons at various conditions as identified in *Figure 2*.

The effect of exposure temperature is prevailing. Heating of the specimens above 500°C initialises the precipitation on the grain boundaries after 1000 hours, but the microstructure in general looks very similar to the as-received material (*Figure 4*). Temperatures above 600°C are causing wider precipitation, mainly on the grain boundaries. After 24 hours, the boundaries are finely decorated but after 1000 hours the precipitation of

the fine carbides can be seen as a cluster on some of the boundaries (see *Figure 4*). Temperatures between 650°C and 750°C create the peak in hardness which is caused by the fine precipitation not only on the grain and annealing twin boundaries but also within the grains.

Typical optical micrographs documenting the microstructural changes in HA230 in the temperature range 750°C and 1050°C for duration of 1000 hours to 30000 hours are shown in *Figure 5*.

The microstructure of the specimens exposed at 750°C contains some primary carbides randomly distributed within the matrix and the fine secondary precipitation on the boundaries and within the grains. At this temperature, the big primary carbides are 'breaking down' (*i.e.* particles which were previously showing no substructure now appear to be no longer homogenous), see *Figure 6*. With increase of the temperature (810°C and 870°C) more and more precipitates are concentrating on the grain boundaries. At 930°C the grain boundary precipitates start to coarsen and primary carbides become more uniform in shape. The lowest hardness of the material at 990°C can be associated with the grain boundary phase coarsening. Rather the phase starts to create 'pools' after long exposures and at 1050°C this 'pool-like' phase creates isolated clusters within the microstructure, see *Figure 5* bottom right.

Figure 6 outlines in detail the transformation of the primary, W-rich, carbide. The 'breaking down' initiates at the edge of the uniform and rounded particles. The Cr-rich phase starts to precipitate in these areas and the two phases can be observed coexisting. As the temperature increases the W-rich carbide is transforming right through to its centre and then again, around 850°C, depending on the duration of exposure, regains its original shape with some cracks in the middle. At the same temperature the Cr-rich phase starts to coarsen. The composition of this phase is complex and varies (transition phase Cr-rich, *Figure 6*). The 'pool-like' phase (*Figure 5*, samples exposed for 20000 and 30000 hours at 1050°C) is very hard and brittle and its composition is mostly the same as that for Cr-rich secondary carbide.

3.3. X-Ray Diffraction

X-Ray diffraction was used to illustrate the phase transformation during the thermal exposure. Initially, analysis was carried out on the bulk material, taking advantage of the non destructive technique, but the necessity to map the phase evolution led to the use of phase extraction in 10% bromine-ethanol solution. The chemical extraction was conducted on as-received material and on the specimens thermally exposed for 3000 hours and 20000 hours at 750°C, 810°C, 870°C, 930°C, 990°C and 1050°C.

The X-Ray radiation is that emitted by copper, with characteristic wavelength (λ) 1.5418Å (Cu). The step size was set to the lowest possible of 0.016° and the speed to 0.15°/min.

The lattice parameter for Haynes Alloy 230 was calculated from the diffractogram and is equal to 3.573Å. Lattice parameter plays an important role in subsequent phase precipitation (*e.g.* influencing distribution and size) [9]. The lattice parameter of pure fcc nickel is 3.523 Å (JCPDS 4-850). Elements in this alloy, such as W, Mo, with atomic radii 1.41 Å, 1.39 Å respectively, distort the lattice and hence shift the lattice parameter.

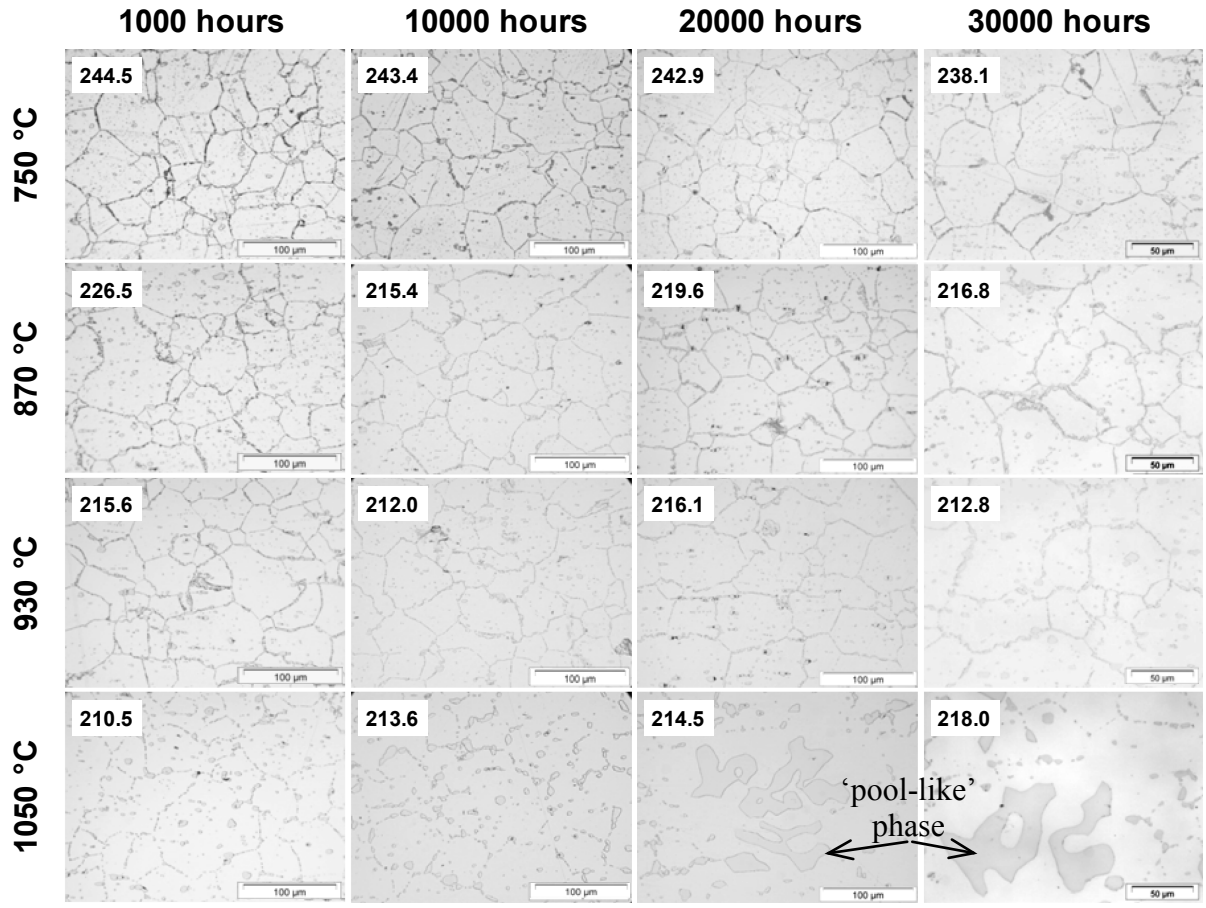

Figure 5 Effects of exposure at temperatures in the range 750°C to 1050°C on the microstructure of HA230 showing average Vickers hardness of each specimen (Hv20).

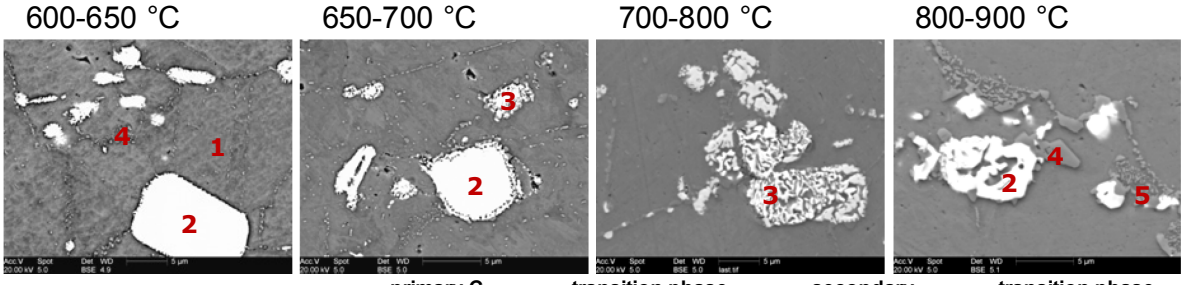

	1 matrix	2 primary C (W-rich)	3 transition phase (W-rich)	4 secondary (Cr-rich)	5 transition phase (Cr-rich)
Ni	58	16	20	9	32
Cr	23	13	33	58	35
W	16	69	43	29	27
Mo	2	6	4	3	5

Figure 6 Transformation of the primary carbide with increase of the temperature and EDX analysis of the phases present in HA230 (average over the set, composition in wt%). The longer duration of exposure, the transformation begins at lower temperature.

The peak assignment determined the second phase in the as-received material as the primary carbide, which has the lattice parameter equal to 10.96Å. This value is very close to the carbide, generally identified as $M_{12}C$ with a lattice parameter equal to 10.95Å and composition Fe_6W_6C (JCPDS 23-1127). The finding contradicts the literature, where this

carbide is usually presented as M_6C type, *e.g.* [2-4, 6-8]. The $M_{12}C$ carbide was found, for example by Tawancy in Hastelloy X at 870°C [10].

The overlay of the XRD spectra for specimens thermally exposed for 20000 hours, *Figure 7*, documents the phase evolution within the temperature range from 750°C to 1050°C.

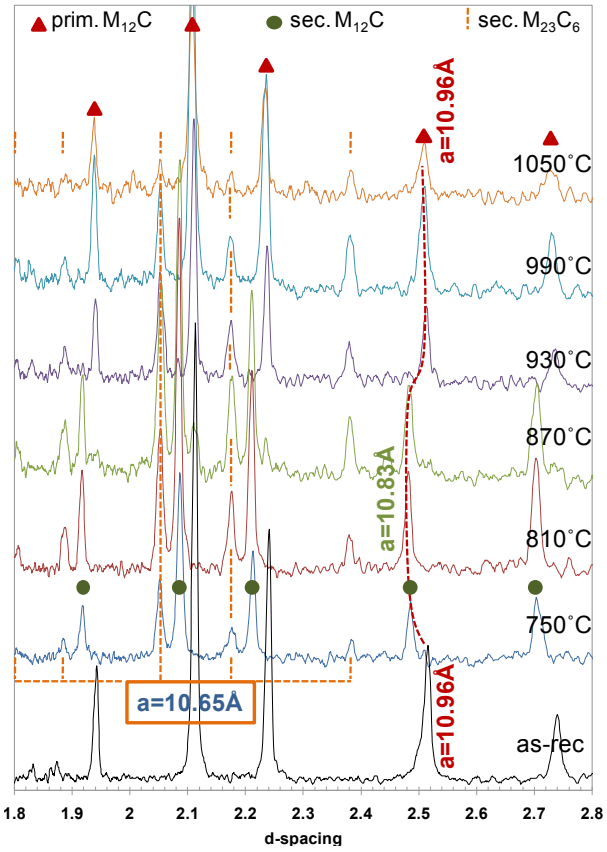

Figure 7 Overlay of XRD spectra acquired on specimens thermally exposed for 20000 hours and the as-received material.

As was mentioned above, the as-received material contains carbide with the lattice parameter equal to 10.96Å, identified as $M_{12}C$. This phase was not detected at 750°C and 810°C. The weak peak appears again at 870°C and the increase of its intensity can be observed with increase of the temperature. The peaks of two secondary phases appear at 750°C. One is the carbide with lattice parameter equal to 10.65Å which corresponds to $M_{23}C_6$ type carbide ($Cr_{23}C_6$ JCPDS 35-783, a=10.66Å), chromium rich. Other peaks correspond to the lattice parameter a=10.83Å and here are called secondary $M_{12}C$ (Co_6W_6C JCPDS 23-939, a=10.89Å), the transition phase tungsten rich. All these carbides are complex and M stands for Cr, W, Ni, Fe, Co. The composition of the carbides is presented in *Figure 6*. Considering the overall intensities of the diffractograms, the $M_{23}C_6$ has the lowest intensity at 750°C but for other temperatures the intensity does not change. Cr-rich phases are sharing the same lattice parameter and the only process occurring is the substitution of the Cr atoms by Ni. The evolution of the secondary $M_{12}C$ is well connected with exposure time.

3.4. Transmission Electron Microscopy

TEM studies have been focused on the identification of phases formed as a result of a long term thermal exposure. The results given here illustrate some of the difficulties. *Figure 8* shows the microstructure of the as-received material with the systems of dislocations on the slip planes, as well as associated with annealing twins within the matrix. There are no precipitates along the dislocations. Some very fine precipitates can be observed along some grain boundaries. These were rich in chromium and are therefore likely to be $M_{23}C_6$ type carbide based on the associated evidence presented earlier.

The exposed specimens were thinned using the Focused Ion Beam technique. This was the most successful approach of those experimented with. Some diffraction patterns have been obtained and evaluated, all of them are from the cubic structures. The lattice parameter of the nickel matrix in HA230 from all the reflections varies reasonably between 3.52 - 3.60 Å.

The estimation of the lattice parameters from other electron diffraction patterns has not provided uniform results. The lattice parameter of the W-rich phase according to the calculation lies between 10.71- 12.45Å and the lattice parameter of the Cr-rich phase lies between 10.27-12.90Å. The results obtained from the electron diffraction patterns for these two phases have such a wide spread of their lattice parameters that there is overlap meaning that a unique identity cannot be achieved. The reason why the measurements from TEMs have the scatter could be, for example hysteresis in the lenses, leading to the actual magnification/ camera length differing from the nominal magnification/ camera length. Consequently it is not possible to distinguish between the same crystal structures with close lattice parameters.

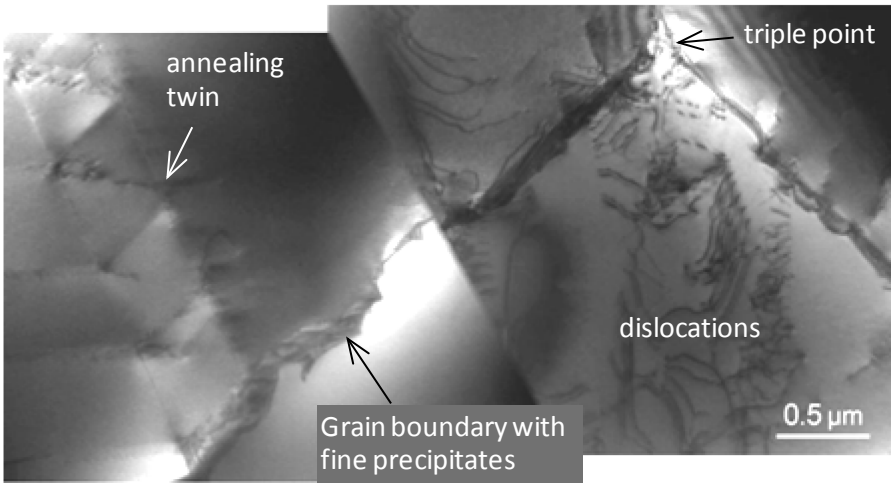

Figure 8 TEM images of the microstructure of the as-received HA230 showing triple point, dislocations, annealing twins and fine precipitation on the grain boundaries.

3.5. Tensile Testing

The effects of high temperature exposure on the mechanical properties of HA230 have been investigated by carrying out room temperature tensile tests on HA230 material exposed for durations of 3000, 10,000 and 20,000 hours at temperatures in the range from 750ºC to 1050ºC. A plot showing the effects of increasing exposure duration and test temperature on the UTS and 0.2% proof strengths of HA230 is presented in *Figure 9*. The results indicate that following an initial increase in tensile strength both the 0.2% PS and UTS decrease linearly with increasing exposure temperature for all three of the exposure durations investigated.

The 0.2%PS and UTS tensile data are shown plotted against the corresponding hardness values for the thermally exposed HA230 material in *Figure 10*. This indicates that although there is some scatter in the results there is a clear correlation between hardness and tensile strength with increases in hardness corresponding to increases in both the 0.2% PS and UTS in the alloy.

The failure mechanism of the tensile fractured specimen was analyzed using scanning electron microscopy. *Figure 11* compares the fractographs of the tensile specimens exposed for 3000 hours in the temperature range from 750ºC to 1050ºC. The failure mechanism in all the samples was intergranular fracture. Triple point wedge cracking is shown in the

micrograph. At low temperatures the faceting can be observed. With increase of the temperature carbide cleavage appears. At the highest temperatures ductile rupture takes place.

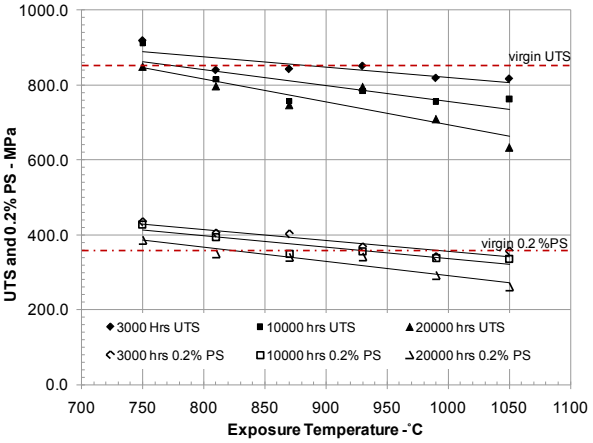

Figure 9 Plot of 0.2% PS and UTS tensile data for HA230 material as a function of temperature for exposure durations of 3K, 10K and 20K hours.

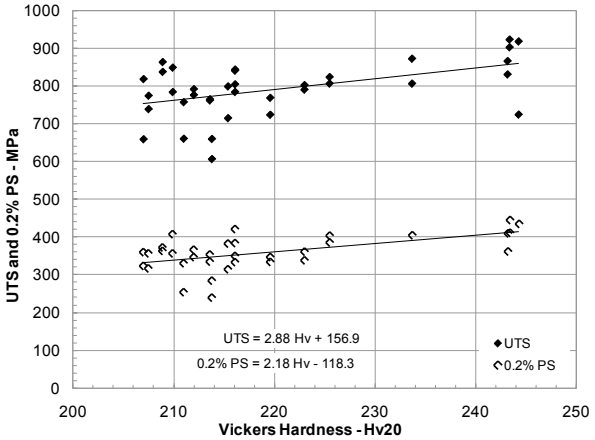

Figure 10 Variation of 0.2% PS and UTS with hardness for thermally exposed HA230.

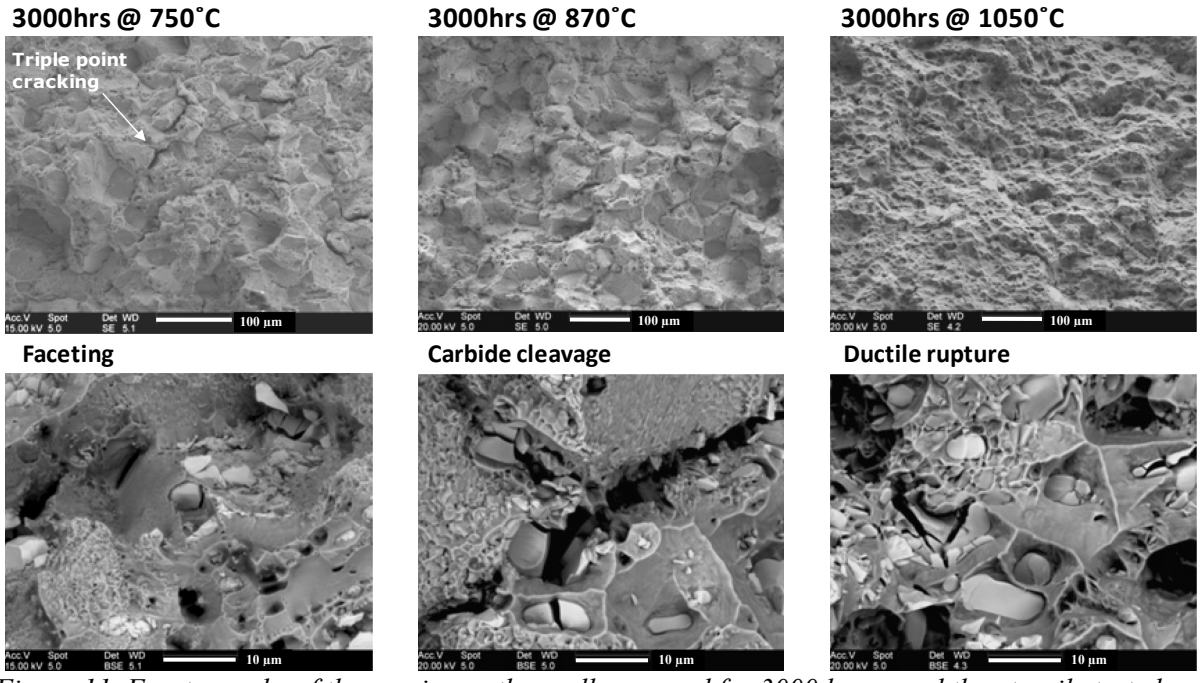

Figure 11 Fractographs of the specimens thermally exposed for 3000 hours and then tensile tested.

Conclusions

The results have demonstrated that a master Hardness v Larson-Miller parametric plot can be generated from the hardness data. A least squares regression analysis has shown that a cubic polynomial gives a good fit to these data with an R^2 value of 0.917. The optimum LMP constant for this set of data was 19.3 but a conventional value of 20 gives almost the same R^2 value. Optical microscopy and FEGSEM studies on thermally exposed HA230 have revealed microstructural factors which can be directly correlated with the observed changes in hardness

due to thermal exposure over the range of temperatures and durations investigated [11]. XRD studies revealed the presence of three precipitating phases in HA230 viz. primary $M_{12}C$ type carbide (~70wt% W), secondary $M_{12}C$ type carbide (~45wt% W) and secondary $M_{23}C_6$ type carbide, with a complex composition over the range of exposures.

Acknowledgements
The authors would like to thank Dr M. Phillips for help with statistical analysis. The authors are also grateful to the COST consortium (Action 538) for facilitating the programme that this study formed part of. Funding from EPSRC and from Siemens is gratefully acknowledged. The EPSRC is thanked for funding the access to the TEM instruments in Oxford Materials under the Materials Equipment Access scheme.

References

1. Haynes International. *HAYNES 230 Alloy Product Brochure, H-3000*. www.haynesintl.com
2. Klarstrom, D.L., The Development of Haynes 230 Alloy, *Corrosion*, p. 407/1-407/12, (1994).
3. Klarstrom, D.L., Heat treatment/Property Relationships for Solid-Solution Strengthened Heat Resisting Alloys, in *1st International Conference on Heat Resistant Materials,* Lake Geneva, (1991).
4. Klarstrom, D.L., The Thermal Stability of a Ni-Cr-W-Mo Alloy, in *NACE Corrosion 94*, (1994).
5. Matthews, S.J., Thermal Stability of Solid Solution Strengthened High Performance Alloys, *Superalloys: Metallurgy and Manufacture*, p. 215-226, (1976).
6. Jordan, C.E., Raserfske, R.K., Castagna, A., Thermal Stability of High Temperature Structural Alloys, Long Term Stability of High Temperature Materials, *Proceedings of TMS Annual Meeting*, p. 55-67, (1999).
7. Whittenberger, J.D., 77 to 1200K Tensile Properties of Several Wrought Superalloys after Long-term 1093K Heat Treatment in Air and Vacuum, *Journal of Materials Engineering and Performance*, **3**(1), p. 91-103, (1994).
8. Vecchio, K.S., Fitzpatrick, M.D., and Klarstrom, D., Influence of Subsolvus Thermomechanical Processing on the Low-Cycle Fatigue Properties of Haynes-230 Alloy, *Metallurgical and Materials Transactions A: Physical Metallurgy and Materials Science*, **26**(3), p. 673-689, (1995).
9. Wang, T., Chen, L.Q., and Liu, Z.K., Lattice parameters and local lattice distortions in fcc-Ni solutions, *Metallurgical and Materials Transactions A: Physical Metallurgy and Materials Science*, **38**(3), p. 562-569, (2007).
10. Tawancy, H.M., Long-term ageing characteristics of Hastelloy alloy X*, Journal of Materials Science*, **18**(10), p. 2976-2986, (1983).
11. Veverkova, J., Strang, A., Marchant, G. R., McColvin, G. M., Atkinson, H. V., High temperature microstructural degradation of Haynes Alloy 230, in *Proceedings of the International Symposium on Superalloys*, p. 479-488 (2008).